Phase Transition, Conformational Disorder, and Chain Packing in Crystalline Long-Chain Symmetrical Alkyl Ethers and Symmetrical Alkenes

Onkar S. Tyagi, Harender S. Bisht, and Alok K. Chatterjee*

Indian Institute of Petroleum (CSIR), Dehradun 248005, India

Received: November 26, 2002; In Final Form: January 6, 2004

The effect of incorporation of a central functionality (ether linkage/olefin double bond) in an *n*-alkane chain on its conformation related properties has been studied using DSC, IR, and wide-angle X-ray scattering (WAXS) techniques. These investigations have also included the influence of alkyl chain length on phase transitions, conformational disorders and chain packing of thus obtained symmetrical alkenes and symmetrical alkyl ethers. The molecules studied involved four symmetrical ethers from 13-oxapentacosane (C_{25}) to 19-oxaheptatriacontane (C_{37}) and three symmetrical alkenes from 15-triacontene (C_{30}) to 19-octatriacontene (C_{38}) having a constant chain length difference of four carbons among them. These compounds are analogues of *n*-alkanes that are known to exhibit a series of chain length-dependent premelt phase transitions. Symmetrical ethers exhibit a more pronounced effect on the depression of both melt and premelt transition temperatures than symmetrical alkenes. The enthalpy of the melt transition showed an increase in the case of symmetrical ethers but a decrease in the case of symmetrical alkenes as compared to the parent *n*-alkanes. However, the enthalpy of premelt transition has decreased for symmetrical ethers but is not altered significantly for symmetrical alkenes. IR absorption spectra of all symmetrical ethers and alkenes revealed the occurrence of almost all common conformational defects of *n*-alkanes at premelt and melt transition temperatures. The WAXS patterns indicate that the crystals of shorter chain (C_{25} and C_{29}) symmetrical ethers may have a helical monoclinic crystal packing, whereas longer chain (C_{33} and C_{37}) symmetrical ethers and all symmetrical alkenes have orthorhombic crystal packing at room temperature (ca. 23 °C). The effect of chain length on conformational properties is more pronounced in symmetrical alkyl ethers than in symmetrical alkenes and *n*-alkanes.

Introduction

The phase behavior of normal alkanes has been studied by many workers[1−6] since the pioneering work of Muller[1] on orientational disorder of *n*-alkane chains around year 1930. These molecules are fascinating for two reasons. First, *n*-alkanes with chain lengths between C_9 and C_{45} (number of carbons in the chain) exhibit a series of thermally induced solid−solid-phase transitions before melting that are attributed to the chain length-dependent conformations of alkyl groups in the crystalline phase. Snyder and co-workers[5,7] have shown, through analysis of infrared (IR) spectra of odd *n*-alkanes obtained at different temperatures, that the number of gauche bonds, hence the concentration of conformational disorders, increases as the temperature of the solid phase is raised to the melting point of the test *n*-alkane. In short-chain *n*-alkanes viz. C_{17}, C_{25}, and C_{36} the conformational disorders appeared discontinuously at the solid−solid phase transitions (usually from orthorhombic to hexagonal packing) just below the melting temperature, whereas in the case of long-chain C_{50} and C_{60} *n*-alkanes these disorders appeared gradually.[7] In these investigations the most prominent and conformationally sensitive IR absorptions have been reported in the C_{17} to C_{45} chain length domain of *n*-alkanes.

Second, simple mixtures of *n*-alkanes and their derivatives show a tendency to mimic the phase behavior of complex systems containing hydrocarbon chains as major constituents, such as petroleum waxes,[8−10] polyethylenes,[11] *n*-alkylammonium salts,[12] *n*-alkanecarboxylic acids,[13] and biological membranes.[14] Their premelting solid−solid transitions have been found to depend on their hydrocarbon chain length.[1,15] Hence, a study of functionalized *n*-alkanes could be useful to understand the phase behavior of complex hydrocarbon systems. Although extensive investigations have been carried out on a large number of pure[5,7] and some multicomponent solid solutions[8] of *n*-alkanes, there is no study to our knowledge on the phase behavior of *n*-alkanes having a central functionality like a double bond or an ether linkage.

The question is whether a conformational disorder similar to that in *n*-alkanes could also occur in long chain symmetrical alkenes and symmetrical alkyl ethers and be also affected by the alkyl chain length. These aspects have been investigated in the present work. For this, we have selected four long chain symmetrical alkyl ethers [viz. 13-oxapentacosane (C_{25}), 15-oxanonacosane (C_{29}), 17-oxatritriacontane (C_{33}), and 19-oxaheptatriacontane (C_{37})] and three symmetrical alkenes [viz. 15-triacontene (C_{30}), 17-tetratriacontene (C_{34}), and 19-octatriacontene (C_{38})]. For describing the chain length of symmetrical ethers above, we have counted the oxygen atom being equivalent to one carbon as C−O and C−C bond lengths are nearly similar.[16] Symmetrical alkene molecules having odd numbers of carbon atoms, however, are not possible. Hence, we have taken alkenes with even carbon numbers for the present work. These molecules are considered to be analogues of *n*-alkanes already studied using IR, X-ray diffraction, and Raman spectroscopies.[5,7,8,17] The molecules were selected so as to produce a constant chain length difference of four carbons to investigate the effect of alkyl chain

* To whom all correspondence should be addressed. Telephone: +91-135-2660113 to 2660116 EPABX 212. Fax: +91-135-2660202 and 2660203. E-mail: alokc@iip.res.in.

10.1021/jp027565x CCC: $27.50
Published on Web 02/06/2004

length on their conformation related properties. Their phase transitions were studied by differential scanning calorimetery (DSC), the crystal structures by wide-angle X-ray scattering (WAXS) at room temperature (ca. 23 °C), and thermally induced conformational changes by IR spectroscopy.

Experimental Section

Materials. The symmetrical alkyl ethers[18] have the general formula $CH_3-(CH_2)_n-O-(CH_2)_n-CH_3$ with $n = 11$, 13, 15, and 17. By counting the oxygen atom equivalent to one carbon atom in the chain, these molecules are abbreviated as C_{25}, C_{29}, C_{33}, and C_{37} ethers, respectively. The symmetrical alkenes[19] have the general formula $CH_3-(CH_2)_n-CH=CH-(CH_2)_n-CH_3$ with $n = 13$, 15, and 17 and are abbreviated as C_{30}, C_{34}, and C_{38} alkenes, respectively. These samples were prepared earlier by other researchers in our laboratory and their synthesis and characterization have been described elsewhere.[18,19] The purity of each compound as determined by gas chromatography was above 99%.

Differential Scanning Calorimetery. A DuPont (model TA-9900) thermal analyzer fitted with a DSC module 910 was employed to measure the temperature and enthalpy of phase transitions of pure compounds. The DSC cell was calibrated using indium metal as a standard reference prior to these measurements. The thermograms were obtained by heating the samples above ambient temperature at 10 °C/min and were analyzed using the software Standard Data version 2.2. The thermograms displayed two peaks above ambient temperature. The major peak was that of melt transition. The premelt transition peak appeared as a shoulder band to the melt transition peak. Nevertheless, their resolution made it clear that there existed a distinct premelting phase. The maximum uncertainty in these measurements was ±0.2 °C for the transition temperature and 2.5% for the enthalpy of transition.

X-ray Diffractometery. The WAXS patterns of samples were obtained at ambient temperature in the range of 2θ from 3° to 45° at a scanning speed of 2°/min using a Rigaku model D/MAX IIIB X-ray diffractometer employing a Cu Kα radiation source operating at 35 kV and 20 mA. The diffraction patterns were digitized and processed by a computer.

Infrared Spectroscopy. IR absorption spectra of neat samples were recorded at different temperatures on a Perkin-Elmer model 1760X FTIR spectrometer equipped with a temperature-stabilized TGS detector and KBr beam splitter. As the conformationally sensitive bands in IR spectra are usually weak, the measurement was done on approximately 250 μm thick films of pure compounds sandwiched between two NaCl plates (IR windows) prepared by heating the samples between these plates to within a few degrees of the melting point of the respective sample. A thermocouple was then attached with the plates, which were fixed in an evacuable, variable temperature double-walled transmission cell model VLT-2. With this arrangement the temperature of the sample could be controlled and measured within an estimated overall accuracy of ±0.5 °C. Before starting the measurements, the sample (placed in above IR cell as described above) was allowed to stay at ambient temperature for 24 h. This was aimed at ensuring the sample molecules to attain their equilibrium conformations. This was confirmed by checking the reproducibility of the sample spectrum. The temperature of the sample was increased in steps from ambient to a few degrees above its melting point, and the spectra were recorded at a resolution of 2 cm^{-1} maintaining the temperature at each step for at least 1 h or until thermal equilibrium was attained, which was confirmed by the reproducibility of consecutive spectra recorded over a period of 30 min. The spectrum was averaged over 20 scans to increase the signal-to-noise ratio.

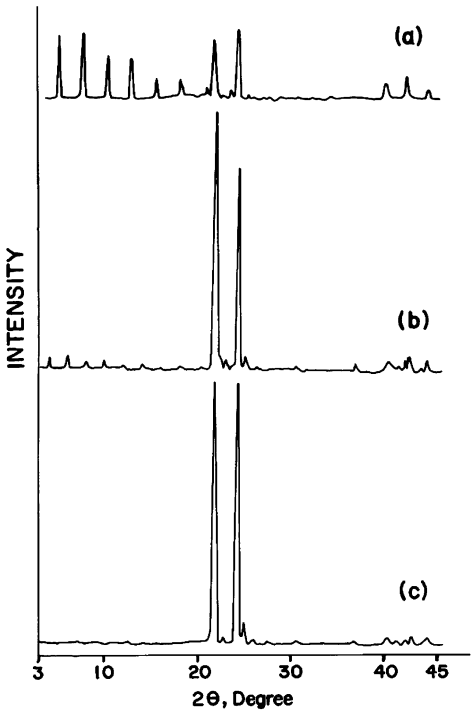

Figure 1. Wide-angle X-ray diffractograms of (a) C_{30}, (b) C_{34}, and (c) C_{38} symmetrical alkenes at ambient temperature (ca. 23 °C).

Results and Discussion

X-ray Diffractometery. *Symmetrical Alkenes.* The WAXS patterns of unoriented samples of symmetrical alkenes are shown in Figure 1. They display two classes of reflections, viz. (i) (00*l*) family at lower 2θ (3−18°) values that arise from the periodicity along the molecular axis and (ii) a pair of strong reflections at 2θ from 20° to 25° that originate from (110) and (200) lattice planes of orthorhombic crystals.[6,20]

These WAXS patterns are similar to those of *n*-alkanes.[21] The relative intensities (I/I_0) of (00*l*) reflections are strong for C_{30} alkene and have been reduced to annulment with increase in alkyl chain length (C_{34} and C_{38} alkenes).

Symmetrical Alkyl Ethers. The WAXS patterns of unoriented samples of symmetrical alkyl ethers are shown in Figure 2. All ethers display very weak intensity ($I/I_0 = 1-6$) of (00*l*) reflections, suggesting that their periodicity along the molecular axis is extremely low. This probably is due to a lower barrier of rotation about the CH_2-O-CH_2 linkage as compared to *n*-alkanes.[16] A number of mixed reflections of variable intensities have also been observed at 2θ from 19° to 25°, i.e., at $d =$ 4.6−3.4 Å. The (110) reflection in shorter chain C_{25} and C_{29} ethers is very weak ($I/I_0 = 3-9$). But, it is the main reflection with $I/I_0 \sim 100$ in the case of longer chain C_{33} and C_{37} ethers. The (200) reflection ($2\theta \sim 24°$) is altogether absent in C_{25} and C_{29} ethers whereas it is present but at very weak intensity in the case of higher (C_{33} and C_{37}) ethers ($I/I_0 = 3$). In addition to the above peaks there are two strong peaks at 2θ about 19° and 23° present only in the WAXS diffractograms of shorter chain C_{25} and C_{29} ethers. Domszy and Booth[22] identified these WAXS peaks, in their study on *n*-alkyl ethers of general formula $CH_3-(CH_2)_n-[OCH_2CH_2]_m-O-(CH_2)_n-CH_3$ where $m = 9$ and $n = 0-25$, as those of (120) (at $2\theta = 19.2-19.4°$) and (112) and (032) (at $2\theta = 23.2-23.6°$) reflections from monoclinic (7/2

TABLE 1: Premelt (T_{pm}) and Melt (T_m) Transition Temperatures (°C) of *n*-Alkanes, Symmetrical Alkyl Ethers, and Symmetrical Alkenes (Accuracy ±0.2 °C)

	n-alkane[a]		ether[b]		alkene[b]	
carbon no.	T_{pm}	T_m	T_{pm}	T_m	T_{pm}	T_m
25	47.2	53.7	30.6 (16.6)	31.7 (22.0)		
26	53.3	56.3				
27	53.2	59.0				
28	58.0	61.2				
29	58.4	63.6	42.4 (16.0)	43.6 (20.0)		
30	62.0	65.4			51.0 (11.0)	52.0 (13.4)
31	62.7	67.9				
32		69.6				
33	67.6	71.3	50.0 (17.6)	51.5 (19.8)		
34	69.6	72.9			59.6 (10.0)	61.1 (11.8)
35	72.1	74.7				
36	74.0	76.1				
37		77.7	60.0 (15.8)	62.1 (15.6)		
38	77.6	79.2			65.2[d] (12.4)	67.6 (11.6)
av depression			16.5 ± 1.0	*c*	11.0 ± 1.0	12.5 ± 1.0

[a] References 3, 30, 31, and 32. [b] The values in parentheses give the depression (ΔT) in T_{pm} and T_m with reference to corresponding *n*-alkane. [c] $\Delta T \sim 0.5$ °C for unit increase in the carbom number of symmetrical alkyl ethers. [d] C_{38} symmetrical alkene has an additional low-temperature transition at 47.8 °C.

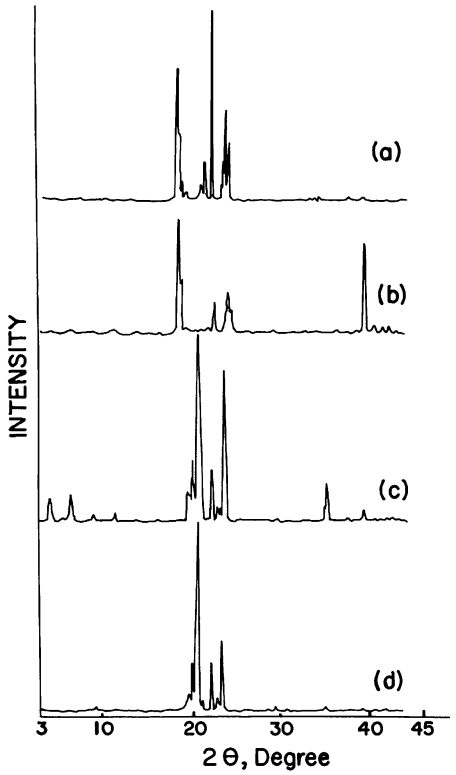

Figure 2. Wide-angle X-ray diffractograms of (a) C_{25}, (b) C_{29}, (c) C_{33}, and (d) C_{37} symmetrical alkyl ethers at ambient temperature (ca. 23 °C).

helical) oxyethylene crystals.[23] In various spectroscopic investigations on *n*-alkyl ethers with $m = 9$ or 15 and n in the range 1−30 Booth and co-workers[22,24] have shown that such oligomers form layered structures in which the oxyethylene central block and the *n*-alkyl end blocks may be crystalline or noncrystalline depending upon the alkyl block length. They suggested that (i) oxyethylene blocks crystallize in helical conformations as in polyoxyethylene and (ii) *n*-alkyl blocks crystallize in planar zigzag conformations as in the *n*-alkanes. Dorset[25] also showed, through a study on hydroxy ended oligomers of formula $CH_3-(CH_2)_{11}-(OCH_2CH_2)_m-OH$ with $m = 1-9$ and $CH_3-(CH_2)_7-(OCH_2CH_2)_m-OH$ with $m = 1-5$ by X-ray and electron diffraction techniques, that the oligomers with $m \geq 4$ crystallized into structures comparable with close packed oxyethylene helices and tilted *n*-alkyl planar zigzags. In Raman spectroscopic studies of $CH_3-(CH_2)_n-(OCH_2CH_2)_m-OH$ with $n = 5, 7, 9, 11$ and $m = 1-8$, Matsuura and Fukuhara[26−29] reported that the oxyethylene blocks of oligomers with $m \geq 4$ crystallized in the helical conformations and the *n*-alkyl blocks essentially with all-trans conformation. It is pertinent to mention here that the reflections similar to those of above monoclinic helical oxyethylenes consisting multiple ether linkages have been observed in the present study even for the molecules consisting single ether linkage, albeit only for shorter length alkyl chain members (C_{25} and C_{29} ethers). This suggests that lower member (C_{25} and C_{29}) symmetrical ethers have possibly monoclinic (7/2 helical) crystal packing whereas higher member (C_{33} and C_{37}) symmetrical ethers have orthorhombic structure at ambient temperature, showing a transition of monoclinic into orthorhombic crystal structure with an increase in alkyl chain length within the series investigated. All symmetrical alkenes studied, on the other hand, have only orthorhombic structure. A few peaks in WAXS are unassigned for both ethers and alkenes, however.

Differential Scanning Calorimetery. All symmetrical ethers and alkenes exhibited two transitions above ambient temperature, i.e., a melting transition (T_m) with one high-temperature premelting transition (T_{pm}). The temperatures of the observed transitions are given in Table 1 and the corresponding enthalpies (ΔH_m and ΔH_{pm}) in Table 2. C_{38} alkene alone showed an additional low-temperature premelting transition at 47.8 °C with an enthalpy of 1.8 kcal mol^{-1}. The corresponding data on *n*-alkanes of similar chain length available in the literature are also included in these tables for comparison. The results reveal that the incorporation of a central functionality (an ether as well as a double bond) in an *n*-alkane chain decreases both its T_m and T_{pm}. This effect is more pronounced in the case of symmetrical ethers than symmetrical alkenes. As compared to the corresponding *n*-alkanes,[3,30−32] the average depression in T_{pm} is about 16 °C for symmetrical ethers and 11 °C for symmetrical alkenes. T_m of symmetrical alkenes also shows a decrease of about 12 °C vis-à-vis *n*-alkanes. The combined effect of alkyl chain length and the substitutions considered on the phase transitions in *n*-alkanes is more vividly illustrated by plotting the transition temperatures versus "carbon number" (Figures 3 and 4). Both T_m and T_{pm} are higher for even *n*-alkanes than odd *n*-alkanes, but this difference is reduced to annulment

TABLE 2: Premelt (ΔH_{pm}) and Melt (ΔH_m) Enthalpies (kcal mol^{-1}) of *n*-Alkanes, Symmetrical Alkyl Ethers, and Symmetrical Alkenes

	n-alkane[a]		ether		alkene	
carbon no.	ΔH_{pm}[b]	ΔH_m	ΔH_{pm}[b]	ΔH_m	ΔH_{pm}[b]	ΔH_m
25	6.8 (49.2)	13.8	1.1 (4.9)	22.2		
26	7.7 (54.2)	14.2				
27	6.5 (45.1)	14.4				
28	8.5 (54.8)	15.5				
29	7.2 (45.6)	15.8	2.0 (7.3)	27.1		
30		16.9[c]			7.4 (62.2)	11.9
33	7.0 (36.8)	19.0	2.5 (8.9)	27.9		
34		19.8[c]			8.0 (65.0)	12.3
36	9.8 (46.2)	21.2				
37		22.0	2.6 (10.3)	25.3		
38		22.6[c]			8.2[d] (51.6)	15.9

[a] References 3, 30, 31, and 32. [b] The values in parentheses are in percent of ΔH_m. [c] Interpolated from the data for even *n*-alkanes. [d] ΔH_m = 1.8 kcal mol^{-1} for additional low-tempearture phase transition observed at 47.8 °C.

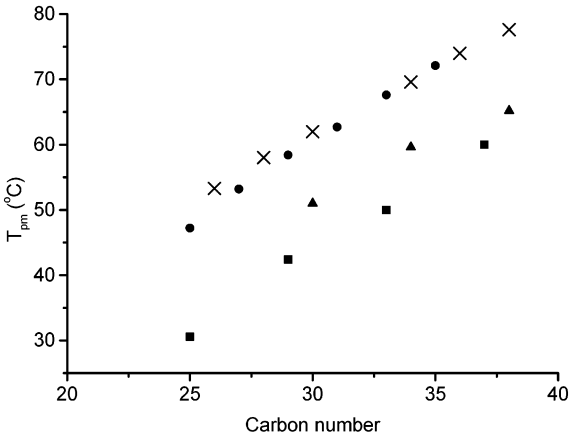

Figure 3. Variation in premelting transition temperature (T_{pm}) of symmetrical alkyl ethers (■), symmetrical alkenes (▲), odd *n*-alkanes (●), and even *n*-alkanes (×) with their carbon number.

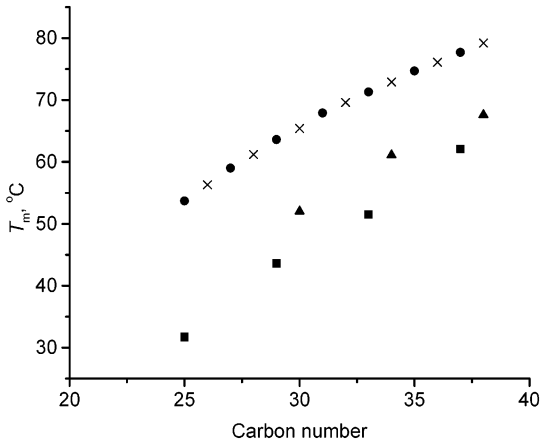

Figure 4. Variation in melting transition temperature (T_m) of symmetrical alkyl ethers (■), symmetrical alkenes (▲), odd *n*-alkanes (●), and even *n*-alkanes (×) with their carbon number.

with an increase in the carbon number of the series. A similar trend is inferred for the present compounds, should one consider the symmetrical ethers being equivalent to odd members and symmetrical alkenes being equivalent to even members of *n*-alkane series, as reasoned earlier in the present manuscript. However, the difference in their melting and premelting transition temperatures is much larger than that reported for *n*-alkanes (Table 1 and Figure 5) arising, most likely, from the

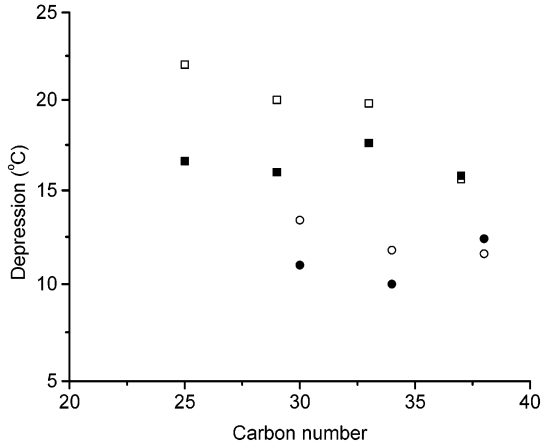

Figure 5. Effect of carbon number on the depression (ΔT) in melting (T_m, open symbol) and premelting (T_{pm}, filled symbol) transition temperatures of symmetrical alkyl ethers (□, ■) and symmetrical alkenes (○, ●) as compared to the corresponding *n*-alkanes.

difference in the crystal packing of test compounds as deduced from WAXS studies.

The effect of alkyl block length on the extent of depression in transition temperatures (ΔT) is pronounced only in the case of T_m of symmetrical ethers (Table 1 and Figure 5). Empirically, it is estimated that a unit increase in the value of *n* in the general formula $CH_3-(CH_2)_n-O-(CH_2)_n-CH_3$ reduces ΔT_m (as compared to that in *n*-alkanes) by 1 °C on average. Further, the difference between T_m and T_{pm} is quite large in the case of lower member *n*-alkanes (i.e., 6.5 °C for *n*-C_{25} and 3.0 °C for *n*-C_{26} homologues), which decreases with an increase in chain length (i.e., 1.6 °C for *n*-C_{38} homologue). However, T_m and T_{pm} are quite close (within 1.3 °C on an average) to each other in all ethers and alkenes studied in this work. This shows that the substitutions considered here involve substantial perturbations on the melting transitions and that they all but eliminate the so-called "hexagonal" or "rotor" or premelting phase II as a distinct phase compared to that of *n*-alkanes, to the extent that it reduces the peak of premelt transition to a shoulder band on the melt transition peak in DSC thermograms.

In general, ΔH_m gradually increases with the alkyl chain length in both ethers and alkenes as in the case of *n*-alkanes (Table 2). Individually, ΔH_m values of symmetrical ethers are higher than those of corresponding *n*-alkanes[3,30−32] whereas ΔH_{pm} are lower. Symmetrical alkenes have the lowest enthalpies of melt transitions. Their premelt enthalpies lie between those of ethers and *n*-alkanes. These results suggest that the molecular arrangements in crystalline phases of symmetrical alkenes are somewhat similar to that of *n*-alkanes whereas the molecules of symmetrical ethers arrange in a manner different from both of them. The melt enthalpy of "C_{37}" symmetrical ether (with longest alkyl block length used in the present work) seems out of line with other values. A probable reason could be the loosening of crystal packing on increasing the alkyl block length, which has been indicated by their WAXS patterns. It is noted that the total entropy change in going from the premelting phase to melt phase on a per "carbon" basis is approximately constant in all three classes of compounds: 10.04 J K^{-1} mol^{-1} in the alkanes, 12.55 J K^{-1} mol^{-1} in the ethers, and 7.95 J K^{-1} mol^{-1} in the alkenes. These values show the effect the substitution has on the conformational freedom of their chains in the melt as discussed in previous sections.

IR Spectroscopy. *Symmetrical Alkenes.* IR spectra of each symmetrical alkene at all temperatures consist of a strong absorption band near 964 cm^{-1} that is characteristic of out-of-

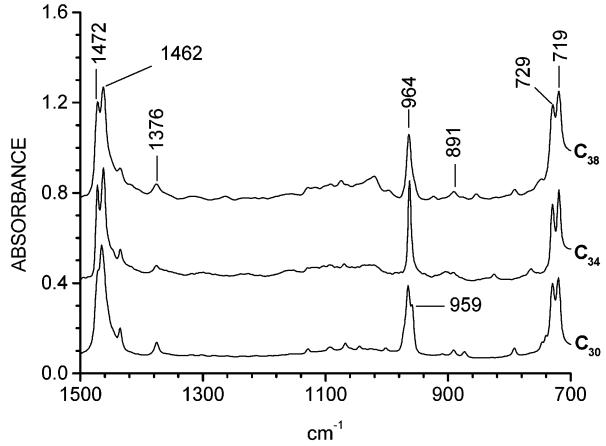

Figure 6. Infrared spectra of C_{30}, C_{34}, and C_{38} symmetrical alkenes in the 1500−700 cm^{-1} region recorded in equilibrium at 23 °C (crystalline phase, at $T \ll T_{pm}$).

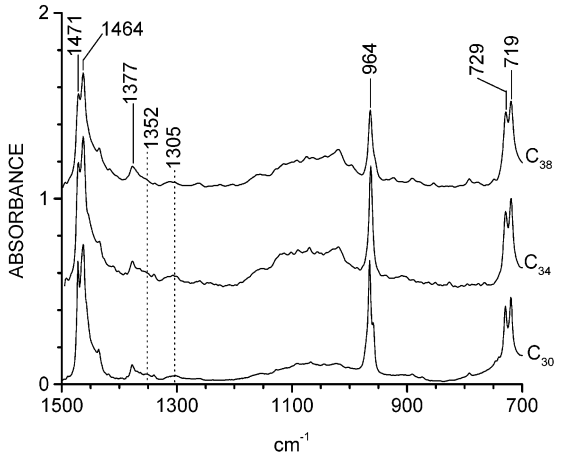

Figure 7. Infrared spectra of C_{30}, C_{34}, and C_{38} symmetrical alkenes in the 1500−700 cm^{-1} region recorded in equilibrium at temperature just below their T_{pm}.

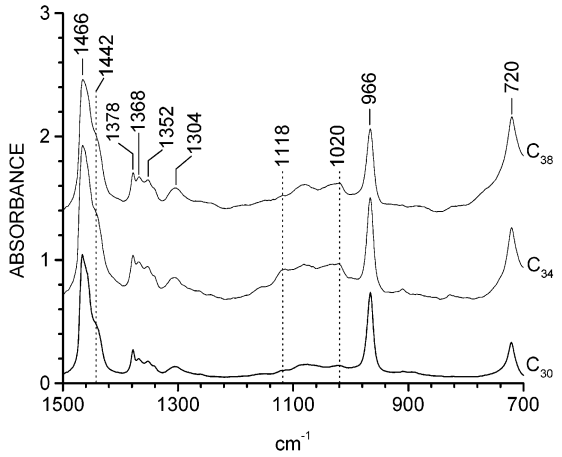

Figure 8. Infrared spectra of C_{30}, C_{34}, and C_{38} symmetrical alkenes in the 1500−700 cm^{-1} region recorded in equilibrium in melt phase ($T > T_m$).

plane C−H deformation in a trans −CH═CH− group (Figures 6−8). This confirms that all symmetrical alkenes retain the trans configuration of the C═C bond even above their melt temperatures. The band near 720−730 cm^{-1}, which is characteristic[33] of $-CH_2-$ rocking mode in an alkyl chain with $CH_3-(CH_2)_n$ ($n \geq 4$), as well as the band at 1462−1472 cm^{-1}, displayed a splitting at temperatures much below T_{pm} (Figure 6). This

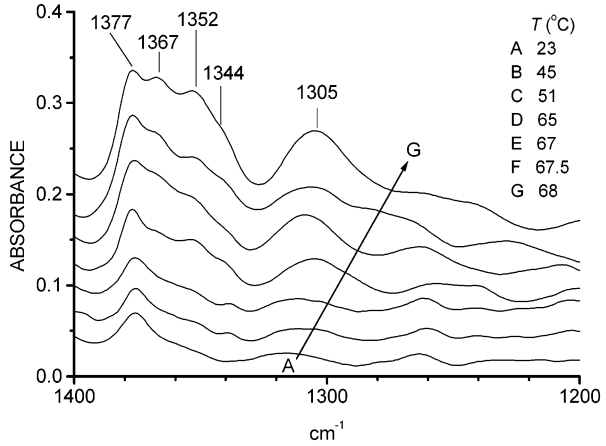

Figure 9. Infrared spectra of C_{38} symmetrical alkenes in conformationally sensitive 1400−1200 cm^{-1} region recorded at different temperatures encompassing its phase transitions.

splitting is indicative of the crystallinity of samples arising due to coupling of intermolecular forces in closely packed orthorhombic crystals, similar to that reported for *n*-alkanes.[5] Figure 6 demonstrates that the increase in alkyl chain length enhances the splitting. The consistencies observed in the IR absorption pattern for each alkene at all temperatures below T_{pm} suggest that the alkenes studied retain their close orthorhombic crystal packing up to almost premelting temperature (Figure 7). As the temperature is raised further to (and above) T_{pm} this splitting vanishes, reducing it to a single peak (at 1464 and 720 cm^{-1}); thus, the loss of orthorhombic crystal packing becomes apparent (Figure 8). A weak absorption due to symmetrical C−H bending in the methyl group is observed near 1376 cm^{-1} for all alkenes at all temperatures. With a rise in temperature there was noticed a gradual increase in the intensity of bands at 1305, 1344, 1352, and 1367 cm^{-1} in the conformationally sensitive region of the IR spectrum, as illustrated in Figure 9. These bands have been assigned to different nonplanar conformational defects as described in Table 3.[5,33] The intensities of these bands, hence the concentration of nonplanar defects, are found to increase with both the alkyl chain length and temperature, as evident from Figures 8 and 9, respectively.

Symmetrical Alkyl Ethers. IR spectra of the longer chain C_{37} alkyl ether in its crystalline state have shown strong peaks at 720−730 cm^{-1} (methylene rocking) and 1463−1472 cm^{-1} (methylene scissoring along with asymmetric C−H bending of methyl) as a splitting that vanished with the decrease in alkyl chain length (Figure 10). In the case of lower member ethers there appeared single strong peaks both at 720 cm^{-1} (with a weak shoulder at the higher frequency side) and at 1472 cm^{-1} (with a smaller peak on lower frequency side). It shows a definitive change in crystal packing in going from C_{37} to C_{25} alykl ethers. On the other hand, shorter chain C_{25} and C_{29} alkyl ethers in their crystalline state have shown a strong sharp absorption near 1135 cm^{-1} due to C−O asymmetric stretch of $-CH_2-O-CH_2-$ group. But, in the case of higher member ethers this band is broad and possesses two lower frequency sidebands at 1125 and 1120 cm^{-1} whose intensities have increased with the chain length of the alkyl block. This alkyl chain length dependent variation in spectral features of the above ethers in their premelt crystalline phase is illustrated in Figure 10. On increasing the temperature these sidebands merge into a single band that shifts to a further lower frequency at 1116 cm^{-1} (Figures 11 and 12). The C−O stretching bands in C_{25} and C_{29} ethers also shift to the same position (1116 cm^{-1}) at temperatures above T_m. As was the case with symmetrical

TABLE 3: Assignments of Relevant IR Absorption Bands (cm^{-1}) to Nonplanar Conformational Defects[5,33]

approximate frequency	description of mode	nonplaner defect
1367	symmetrical CH_2 wagging with respect to the center of trans bond	-gtg- or -gtg′- (kink)
1352	localized CH_2 wagging of double gauche	double gauche, -gg-
1344	localized CH_2 wagging of end gauche	end gauche, eg-
1305	asymmetrical CH_2 wagging with respect to the center of trans bond	-gtg- or -gtg′- (kink)

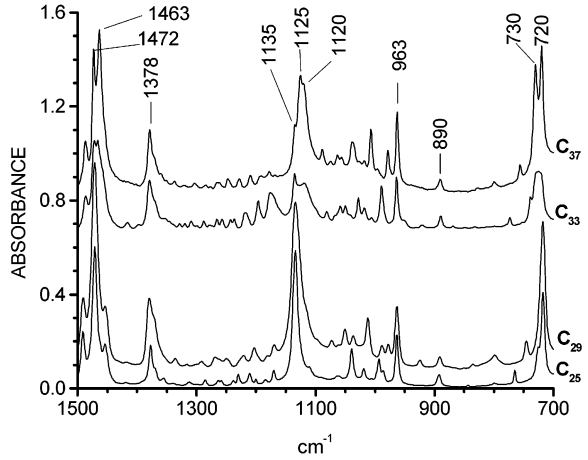

Figure 10. Infrared spectra of C_{25}, C_{29}, C_{33}, and C_{37} symmetrical alkyl ethers in the 1500−700 cm^{-1} region recorded in equilibrium at 23 °C (crystalline phase, at $T \ll T_{pm}$).

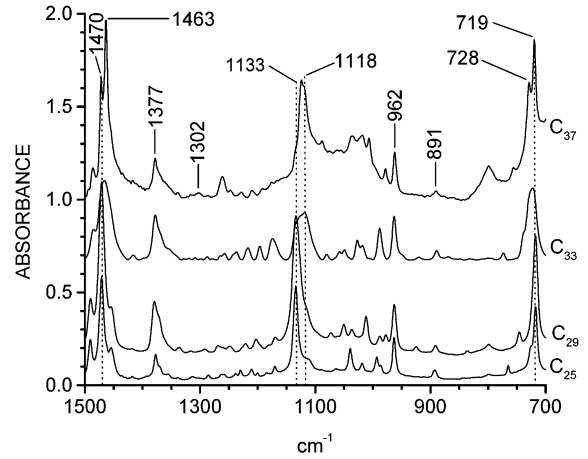

Figure 11. Infrared spectra of C_{25}, C_{29}, C_{33}, and C_{37} symmetrical alkyl ethers in the 1500−700 cm^{-1} region recorded in equilibrium at temperature just below their T_{pm}.

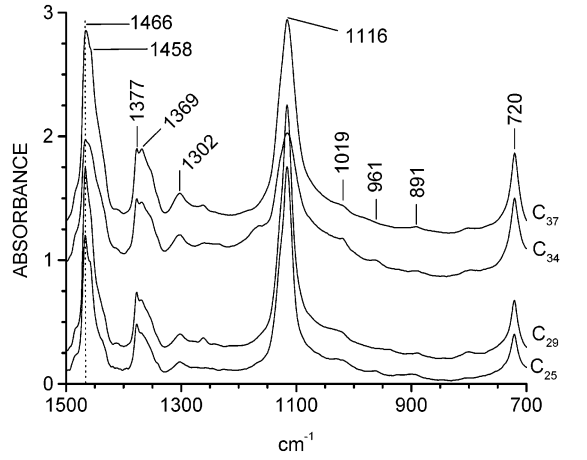

Figure 12. Infrared spectra of C_{25}, C_{29}, C_{33}, and C_{37} symmetrical alkyl ethers in the 1500−700 cm^{-1} region recorded in equilibrium in melt phase ($T > T_m$).

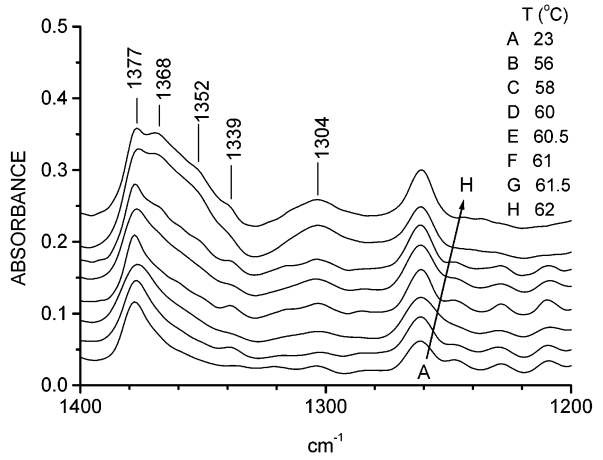

Figure 13. Infrared spectra of C_{37} symmetrical alkyl ether in the conformationally sensitive 1400−1200 cm^{-1} region recorded at temperatures encompassing its phase transitions.

alkenes, the splitting in both the bands at 720−730 and 1467−1472 cm^{-1} vanished also with an increase in temperature, reducing both the splitting to single peaks at $T \sim T_{pm}$ even for the C_{37} alkyl ether. These results demonstrate the predominant effect of both the central functionality and the alkyl chain length on the crystal structure of ethers investigated. The above IR spectral features support the WAXS results, showing that the higher member C_{37} alkyl ether has an orthorhombic packing in the crystalline phase below T_{pm}, which is lost at higher temperatures, as was the case with symmetrical alkenes, whereas the C_{33} alkyl ether probably has a pseudo-orthorhombic packing. A medium intensity band at 963 cm^{-1}, which was observed for all ethers at temperatures below T_{pm}, was reduced to annulment at T_m. However, it could not be assigned. The absorption band near 890 cm^{-1} due to the methyl rocking mode has broadened near T_m. All absorption bands in the conformationally sensitive region (1300−1370 cm^{-1}) described for symmetrical alkenes in previous section have also been seen in the spectra of ethers with rise in temperature (cf. Figure 13). A few of the bands observed in IR spectra of both alkenes and ethers, however, remain unassigned.

Conclusion

All symmetrical C_{30} to C_{38} alkenes and symmetrical C_{33} and C_{37} alkyl ethers have orthorhombic crystal packing at room temperature. It is suggested that C_{25} and C_{29} alkyl ethers may have monoclinic (7/2 helical) type crystal packing. The trans configuration of the double bond in alkenes remains unchanged even above the melting temperature. The incorporation of ethereal oxygen as well as a double bond in the center of an *n*-alkyl chain induces depressions in both melt and premelt transition temperatures, the influence of the former type of functionality being much greater than that of the latter type. Both symmetrical alkenes and ethers show nonplanar conformational defects of *n*-alkanes in high-temperature phases. Their concentration increases with an increase in alkyl block length.

Acknowledgment. We thank the Director, Indian Institute of Petroleum, Dehradun, for permission to publish this paper.

We are grateful to the referees for valuable comments and suggestions. Acknowledgments are also due to (the late) Mr. S. Suresh for technical help in recording X-ray diffractograms. H.S.B. is thankful to the Council of Scientific and Industrial Research, New Delhi, for award of a research fellowship to him.

Supporting Information Available: Table of X-ray scattering data. This material is available free of charge via the Internet at http://pubs.acs.org.

References and Notes

(1) Muller, A. *Proc. R. Soc., London, Ser. A.* **1932**, *138*, 514.
(2) Smith, A. E. *J. Chem. Phys.* **1953**, *21*, 2229.
(3) Schaerer, A. A.; Busso, C. J.; Smith, A. E.; Skinner, L. B. *J. Am. Chem. Soc.* **1955**, *77*, 2017.
(4) Sullivan, P. K.; Weaks, J. J. *J. Res. Natl. Bur. Stand.* **1970**, *A74*, 203.
(5) Maroncelli, M.; Qi, S. P.; Strauss, H. L.; Snyder, R. G. *J. Am. Chem. Soc.* **1982**, *104*, 6237−6247.
(6) Strobl, G.; Ewen, B.; Fisher, E. W.; Piesczek, W. *J. Chem. Phys.* **1974**, *61* (12), 5257−5264.
(7) Kim, Y; Strauss, H. L.; Snyder, R. G. *J. Phys. Chem.* **1989**, *93* (21), 7520−7526.
(8) Clarell-Grunbaum, D.; Strauss, H. L.; Snyder, R. G. *J. Phys. Chem. B* **1997**, *101*, 335−343.
(9) Srivastava, S. P.; Handoo, J.; Agarwal, K. M.; Joshi, G. C. *J. Phys. Chem. Solids* **1993**, *54*, 639.
(10) Tiwari, G. B.; Tyagi, O. S.; Srivastava, S. P.; Pandey, D. C.; Goyal, S. K.; Kapoor, V. B. *Ind. J. Chem. Technol.* **1997**, *4*, 29−22.
(11) Bassett, D. C.; Turner, B. *Nature (London), Phys. Sci.* **1972**, *240*, 146.
(12) Tsau, J.; Gilson, D. F. R. *J. Phys. Chem.* **1968**, *72*, 4082.
(13) Barr, M. R.; Dunell, B. A.; Grant, R. F. *Can. J. Chem.* **1963**, *41*, 1188.
(14) Nagle, J. F. Annu. *Rev. Phys. Chem.* **1980**, *31*, 157.
(15) Doucet, J.; Denicolo, I.; Craievich. A.; Collet, A. *J. Chem. Phys.* **1981**, *75*, 5125.
(16) Mark, H. F. *Chemtech* **1984**, *4*, 220.
(17) Snyder, R. G.; Maroncelli, M.; Strauss, H. L. *J. Am. Chem. Soc.* **1983**, *105*, 133−134.
(18) Chaturvedi, P. K.; Murthy, P. S. N.; Srivastava, S. P.; Joshi, G. C. *Ind. J. Technol.* **1990**, *28*, 39.
(19) (a) Singh, S. K. PhD Thesis, H. N. B. Garhwal University, Srinagar (Garhwal), Uttranchal, India, 1991. (b) Singh, S. K.; Murthy, P. S. N.; Joshi, G. C. *Tetrahedron Lett.* **1992**, *33* (17), 2419.
(20) Ebert, L. B.; Scanlon, J. C.; Mills, D. R. *Petroleum Prepr.* **1982**, 1353.
(21) Kitaigorodskii, A. I. *Organic Chemical Crystallography*; Consultant Bureau: New York, 1961.
(22) Domszy, R. C.; Booth, C. *Makromol. Chem.* **1982**, *183*, 1051.
(23) Tadokoro, H. *Structure of Crystalline Polymers*; Wiley: New York, 1979; Chapter 4.
(24) Teo, H. H.; Swales, T. G. E.; Domszey, R. C.; Heatley, F.; Booth, C. *Makromol. Chem.* **1983**, *184*, 861.
(25) Dorset, D. L. J. *Colloid Interface Sci.* **1983**, *96*, 172.
(26) Matsuura, H.; Fukuhara, K. *J. Phys. Chem.* **1986**, *90*, 3057.
(27) Matsuura, H.; Fukuhara, K. *J. Phys. Chem.* **1987**, *91*, 6139.
(28) Matsuura, H.; Fukuhara, K. *J. Mol. Struct.* **1988**, *189*, 249.
(29) Matsuura, H.; Fukuhara, K.; Masatoki, S.; Sakakibara, M. *J. Am. Chem. Soc.* **1991**, *113*, 1193.
(30) Broadhurst, M. G. J. *Res. Natl. Bur. Stand. Sect. A* **1962**, *66* (3), 241.
(31) Turner, W. R. *Ind. Eng. Chem. Prod. Res. Dev.* **1971**, *10* (3), 238.
(32) Flory, P. J.; Vrij, A. *J. Am. Chem. Soc.* **1963**, *85*, 3548.
(33) Snyder, R. G. *J. Chem. Phys.* **1967**, *47* (4), 1316.